

# Kinetic energy in sprinkler irrigation: different sources of drop diameter and velocity

by

Bautista-Capetillo C<sup>1\*</sup>, Zavala M<sup>1</sup>, Playán E<sup>2</sup>

## Abstract

Sprinkler kinetic energy has been linked to a number of problems in irrigated fields. This work presents the characterization of sprinkler drop kinetic energy and specific power from low-speed photographic drop data using a commercial impact sprinkler and three operating pressures. The spatial variability of specific power ( $\text{W m}^{-2}$ ) was assessed for different sprinkler spacings, showing different patterns in rectangular and triangular spacings. The specific power uniformity coefficient ranged from 38 % to 77 %, depending on sprinkler spacing and operating pressure. An attempt was made to characterize specific power from estimated (measured diameter and estimated velocity) and simulated data (using a ballistic model). While estimated data produced adequate results, simulated data resulted in a large overestimation. Discrepancies in kinetic variables between measured and simulated drop data permit to conclude that it is important to continue experimental drop characterization efforts as well as sprinkler simulation model development.

**Keywords:** kinetic energy, drop diameter, drop velocity, indoor experiments, sprinkler irrigation, low-speed photography, disdrometer.

---

<sup>1</sup> Planeación de Recursos Hidráulicos, Universidad Autónoma de Zacatecas, 98000 Zacatecas, Mexico.

<sup>2</sup> Departamento Suelo y Agua., Estación Experimental de Aula Dei, CSIC. P. O. Box 202. 50080 Zaragoza, Spain.

\* Corresponding author: [baucap@uaz.edu.mx](mailto:baucap@uaz.edu.mx)

## **Introduction**

The design of a solid-set sprinkler irrigation system is based on the adequate selection of the irrigation hardware, the sprinkler layout and riser elevation, and the operating conditions. Among these, the nozzle operating pressure determines drop size distribution and therefore the sprinkler water application pattern, including the wetted radius. Drop characterization refers to the statistical determination of drop static and dynamic properties namely drop diameter, the module of drop velocity and the angle of drop trajectory relative to a horizontal plane. Drop characterization is commonly performed at different distances from the sprinkler, and near the soil surface. This technique permits to understand the behavior of a sprinkler at a certain pressure (Kincaid et al. 1996) and to estimate the water application pattern using ballistic simulation models (Fukui et al. 1980). Drop characterization is also required to develop analytical models of wind drift and evaporation losses. In these models evaporation affects individual drops, modifying their diameter, aerodynamic drag and velocity along their trajectory from the sprinkler to the soil surface (De Wrachien and Lorenzini 2006). Despite its obvious importance, the application of drop characterization to irrigation practice is severely limited by experimental difficulties and by the need to experiment with each combination of sprinkler model, nozzle size and operating pressure.

Drop characterization is needed to evaluate the relationship between the irrigation system design and management, the soil and the crop, through the effect of drop impact on soil structure. A number of researchers have found strong relations between the kinetic energy of water drops and the change in physical properties of the soil surface. Thompson and James (1985) analyzed the increase in hydraulic resistance of the soil surface layer as the

drop kinetic energy per unit soil surface area increased. These authors also reported a decrease in soil infiltration with increasing rainfall intensity, kinetic energy per water droplet and water droplet energy flux. In their experimental work, Thompson and James (1985) used a Warden silt loam soil and applied precipitation at a rate of  $30 \text{ mm h}^{-1}$  with an average drop diameter of 3 mm. They found infiltration depths (prior to ponding) of 120 mm and 40 mm for drop kinetic energies of  $67.9 \cdot 10^{-7} \text{ J}$  and  $1,206 \cdot 10^{-7} \text{ J}$ , respectively. They also experimented with the same drop kinetic energy ( $1,206 \cdot 10^{-7} \text{ J}$ ) and different rainfall intensities ( $30 \text{ mm h}^{-1}$  and  $150 \text{ mm h}^{-1}$ ), and found that infiltration decreased 51 % for the highest rainfall intensity (infiltration rate of 40 mm *vs.* 22 mm, respectively).

Kohl et al. (1985) reported an increase in kinetic energy per unit volume of discharged water ( $\text{J L}^{-1}$ ) when the operating pressure was reduced. Similar results were obtained by Basahi (1998), when determining the specific power ( $\text{W m}^{-2}$ ) of experimental water drops impacting on a surface. This author obtained fluxes of 0.047, 0.038 and  $0.025 \text{ W m}^{-2}$  for pressures of 69, 103 and 138 kPa, respectively. For an isolated impact sprinkler with a nozzle diameter of 3.97 mm and an operating pressure of 400 kPa, Kohl et al. (1985) determined sprinkler kinetic energy per unit volume of water at different distances from the sprinkler. They obtained values of 4, 7, 11, and  $17 \text{ J L}^{-1}$  for distances of 3, 6, 9, and 12 m, respectively. These authors identified kinetic energy peak values of  $25 \text{ J L}^{-1}$ , but only in small portions of the wetted area.

Mohammed and Kohl (1987) discussed previous experiments performed by Duley (1939) and Ellison (1947), whose results showed that water drops destroyed surface aggregates and gradually formed a surface seal characterized by much lower hydraulic conductivity than the original soil surface. Surface seal development has been linked to rainfall energy

and intensity, as well as to soil aggregate stability (Thompson and James 1985; Lehrs and Kincaid 2010).

Wind velocity has been shown to have direct influence on drop kinetic energy. Based on a simulation model, Kincaid (1996) presented in a graph the relationship between wind velocity and kinetic energy for an impact sprinkler with a 3.8 mm diameter nozzle and operating at 400 kPa. The sprinkler kinetic energy for a set of drops traveling in no wind conditions was  $12 \text{ J L}^{-1}$ . For wind velocities of 5 and 10  $\text{m s}^{-1}$ , sprinkler kinetic energies were 25 and  $58 \text{ J L}^{-1}$ , respectively.

Regarding soil erosion, Basahi (1998) used a piezoelectric film sensor to show that the erosive energy increases with decreased operating pressure, as well as with increased irrigation time. The average experimental values for soil erosion rate reported by this author (for an irrigation time of 100 min) were 2.3, 2.1, and  $1.2 \text{ Mg ha}^{-1} \text{ h}^{-1}$  for operating pressures of 69, 103, and 137 kPa, and application rates of 32, 33 and  $39 \text{ mm h}^{-1}$ , respectively. When the soil was exposed to an irrigation time of 150 min, the average experimental erosion rates were 5.9, 3.0, and  $1.4 \text{ Mg ha}^{-1} \text{ h}^{-1}$  (for the same operating pressures and application rates).

An adequate characterization of drops emitted by a sprinkler irrigation system permits evaluation of the kinetic energy with which drops impact the soil surface. Drop characteristics depend on a number of factors, including the type of sprinkler and nozzle design and diameter, the operating pressure and the environmental conditions. Different experimental methods for drop characterization have been reported in the literature since the 19<sup>th</sup> century (Wiesner 1895). However, a number of experimental approaches have been reported since the 1990s. The most relevant techniques used for drop diameter

determination are: stain method (Magarvey 1956), momentum method (Joss and Waldvogel 1967), oil immersion method (Eigel and Moore 1983), flour method (Kohl and DeBoer 1984), optical methods (Hauser et al. 1984; Kincaid et al. 1996; Montero et al. 2003; King et al. 2010) and photographic methods (Jones 1956; Sudheer and Panda 2000; Salvador et al. 2009). These techniques have been applied to either rainfall or sprinkler irrigation drop diameter determination (Cruvinel et al. 1996; Cruvinel et al. 1999; Salles et al. 1999; Sudheer and Panda 2000; Montero et al. 2003; Bautista-Capetillo et al. 2009).

Routine, fast drop diameter and velocity determinations can be currently performed using laser beams (Kincaid et al. 1996). An alternative technique is based on the attenuation of a luminous flow -such as the disdrometer technique- (Montero et al. 2003; King et al. 2010). This is a simple technique that can be used even in outdoor conditions. Bautista-Capetillo et al. (2009) analyzed data quality resulting from a disdrometer (model ODM 470, Eigenbrodt, Königsmoor, Germany). These authors confirmed the quality of drop diameter measurements, and concluded that velocity estimates could not be obtained from this particular device. Low-speed photography (Salvador et al. 2009) has recently been proposed as a simple method to measure sprinkler drop diameter, velocity and vertical angle. These experimental determinations are commonly performed in no-wind conditions, since drop dynamics are strongly influenced by wind speed and direction, and these variables continuously fluctuate. Wind tunnel experiments have not been reported in sprinkler irrigation.

Salvador et al. (2009) presented an empirical logarithmic equation predicting drop velocity (near the soil surface) from drop diameter. The equation was derived from experiments performed in Zaragoza, Spain for an isolated sprinkler installed at an elevation of 2.15 m

with a 4.8 mm nozzle at 200 kPa. Bautista-Capetillo et al. (2009) revised the equation, adding an independent data set obtained at pressures of 200, 300 and 400 kPa. The proposed equation was:

$$V = 2.28 \ln(d) + 3.25 \quad [1]$$

Where:

$d$  is drop diameter (m); and

$V$  is the module of drop velocity ( $\text{m s}^{-1}$ ).

This equation explained 89 % of the variability in the data set, and resulted in a standard error of  $0.43 \text{ m s}^{-1}$  in the range of velocities  $1\text{-}8 \text{ m s}^{-1}$ , approximately.

In a number of sprinkler droplet characterization studies, drop velocity was estimated using classical physics. Seginer (1965) proposed a procedure based on ballistic concepts to estimate the tangential velocity of water drops with diameters of 1-6 mm. This methodology was used by Kohl et al. (1985), Mohammed and Kohl (1987) and Kincaid (1996), among others. Ballistic sprinkler simulation models take as basic input the sprinkler and nozzle model and elevation, the operating pressure and the wind velocity vector (Fukui et al. 1980; Vories et al. 1987; Carrión et al. 2001; Playán et al. 2006). Model calibration and validation is based on: 1) the experimental radial water application pattern obtained at no-wind conditions; and 2) A number of experiments performed under different wind conditions in which a matrix of collectors is located under a given sprinkler spacing (the space between four sprinklers in a rectangular or triangular arrangement). Model calibration involves the determination of the drop diameter distribution minimizing the error in the simulation of the radial water application pattern. Once

calibrated and validated, a ballistic model can simulate the spatial distribution of water application, drop diameters and velocities under windy conditions. Burguete et al. (2007) reported on the current degree of empiricism of sprinkler simulation models, resulting on the introduction of empirical parameters. As a consequence, performing drop characterization from ballistic models can be subjected to relevant errors.

This paper reports on the kinetic energy emitted by an irrigation sprinkler in the absence of wind (indoor conditions), using drop diameters and velocities obtained from low-speed photographs. Maps of specific power and coefficients of uniformity are presented as a methodological contribution to decision making in sprinkler system design and management. Finally, two additional sources of specific power data are assessed: 1) measured drop diameter and estimated drop velocity from diameter measurements; and 2) simulated drop diameter and velocity using a ballistic model. The application of these data sources to the estimation of specific power is assessed.

## **Materials and methods**

### **Experimental Data**

Bautista-Capetillo et al. (2009) reported on an experiment performed on an isolated irrigation impact sprinkler in indoor conditions. The sprinkler model was VYR35 manufactured in brass (VYRSA, Burgos, Spain). The sprinkler nozzle was 4.8 mm in diameter and had an inclination angle of 26° respect to a horizontal line. Drops were characterized at an elevation of 0.50 m below the sprinkler nozzle. Three operating pressures (200, 300 and 400 kPa), and four distances from the sprinkler (3, 6, 9 and 12 m) were used for drop characterization using low-speed photography (Salvador et al. 2009). Wetted radii of 14.40, 15.60 and 16.80 m and flow rates of 1,235, 1,500 and 1,760 L h<sup>-1</sup> were obtained for operating pressures of 200, 300 and 400 kPa, respectively. Drop diameter, vertical angle and velocity were measured in a total of 1,229 drops identified in images obtained with a standard reflex digital camera. More experimental details can be obtained at the original reference. Additionally, the complete drop characterization data set can be obtained at [www.eead.csic.es/drops](http://www.eead.csic.es/drops).

### **Kinetic energy and power**

Drop kinetic energy ( $E_{kd}$ , J) was determined according to Kohl et al. (1985) as:

$$E_{kd} = \frac{1}{12} \pi d^3 \rho_w V^2 \quad [2]$$

Where  $\rho_w$  is water density (kg m<sup>-3</sup>), and the other terms as defined previously

The sprinkler kinetic energy applied to a certain domain  $\Omega$  per unit volume of water application ( $E_{k\Omega}$ , J L<sup>-1</sup>) can be determined from the total drop kinetic energy and the total volume of a given set of drops of size  $n$  (King and Bjorneberg 2010).

$$E_{k\Omega} = \frac{\sum_{i=1}^n E_{kd_i}}{1000 \sum_{i=1}^n \frac{1}{6} \pi d_i^3} \quad [3]$$

Depending on the selection of the domain (and therefore of the set of drops),  $E_{k\Omega}$  can be determined for all the area irrigated by a sprinkler or for a sprinkler irrigated subarea (i.e., a square domain or a circular crown). While  $E_{kd}$  is useful to characterize individual drops,  $E_{k\Omega}$  conveys information on the agronomic effects (soil loss due to erosion and reduction in the infiltration rate) resulting from sprinkler irrigation in a certain area.

$E_{k\Omega}$  can be combined with the precipitation falling in the domain to determine kinetic power:

$$P_{k\Omega} = E_{k\Omega} R_{\Omega} \quad [4]$$

Where:

$P_{k\Omega}$  is the kinetic power applied to a domain (W); and

$R_{\Omega}$  is the precipitation rate applied to a domain (L s<sup>-1</sup>)

Switching from kinetic energy to kinetic power is important in the context of sprinkler irrigation, since the irrigation time (per irrigation event, per season...) is an important management variable. Once power is determined, multiplying it times a certain irrigation duration (often expressed in hours) will result in the kinetic energy of a given irrigation event or a set of irrigation events.

The specific power ( $\delta_p$ ,  $W m^{-2}$ ) is the flux of kinetic energy per unit area and time, and can be determined as:

$$\delta_p = E_{k\Omega} R \quad [5]$$

Where  $R$  is the precipitation rate ( $L m^{-2} s^{-1}$ ).

Specific power is useful to assess the effect of sprinkler irrigation on cropped soils, and permits comparisons between sprinkler irrigation systems. Specific power has been related to the modification of the physical properties of the soil surface (Kincaid, 1996).

### **Ballistic theory applied to sprinkler irrigation systems**

Different models have been developed in the last decades to simulate sprinkler irrigation (Fukui et al. 1980; Vories et al. 1987; Carrión et al. 2001). These models take into account the effect of wind as a major determinant of irrigation uniformity for a given sprinkler hardware and operating pressure. In the models, a sprinkler is considered as a device emitting drops of known diameters. Drop trajectory (from the nozzle to the soil surface or crop canopy) is determined by the application of ballistic theory. According to ballistics, drop movement is influenced by the initial velocity vector, the gravitational force (acting in the vertical direction), the wind vector and the aerodynamic drag (applied in the opposite direction to the relative drop movement) (Vories et al. 1987; Carrión et al. 2001; Dechmi et al. 2004a; Dechmi et al. 2004b).

Due to the complexities derived from the analysis of the sprinkler jet breakup, the following simplifications are commonly included in ballistic sprinkler models (Carrión et al. 2001): 1) the jet disintegrates into drops of different diameters at the nozzle; 2) drops move independently from each other; 3) the drag coefficient is constant and it is

commonly calculated independent of sprinkler elevation from the soil surface, jet vertical angle, wind speed and nozzle diameter; and 4) drops of different diameters land at different distances from the sprinkler; all drops landing at a certain distance from the sprinkler have the same diameter.

Fukui et al. (1980) presented the set of three differential equations governing drop trajectory in a three-dimensional Cartesian system. These equations relate drop acceleration to air and water density, the drag coefficient ( $C_d$ ) and wind velocity. The drag coefficient can be determined as a function of the Reynolds number, following different formulations (Okamura 1968; Fukui et al. 1980; Park et al. 1982; Kincaid 1996). Alternatively,  $C_d$  can be determined as a function of the operating pressure, the drop diameter, the equivalent nozzle diameter and the discharge coefficient of the nozzle (Li and Kawano 1995):

$$\begin{aligned} C_d &= 51.46 H^{0.179} d^{1.181} D_e^{1.936} C^{3.318} \text{ for } d \leq 2 \text{ mm;} \\ C_d &= 0.3 \text{ for } d > 2 \text{ mm} \end{aligned} \quad [6]$$

Where:

$H$  is the operating pressure (kPa);

$D_e$  is the equivalent nozzle diameter (mm), determined as:  $D_e = \frac{4\alpha}{\beta}$ ;

$\alpha$  is the area of nozzle outlet section (mm<sup>2</sup>);

$\beta$  is the wetted perimeter of nozzle outlet section (mm); and

$C$  is the nozzle discharge coefficient.

In order to solve the ballistic equations (Fukui et al. 1980), a fourth order Runge-Kutta numerical integration method (Press et al. 1988) was used. The equations were solved for discrete time intervals (0.005 s). In the experimental conditions, the solution for a given drop diameter and operating pressure consists of the values of distance from the sprinkler and  $V$  at the point where drop elevation from the nozzle is equal to -0.5 m (the relative elevation of the drop characterization points, with elevations measured upwards being positive). Since the experiments were performed indoors, windless conditions were assumed in all cases.

### **Determining specific power radial curves**

Equations were built to estimate  $\delta_p$  as a function of distance from the sprinkler for operating pressures of 200, 300 and 400 kPa. Different data sources were used:

#### *Experimentally measured drop diameter and velocity data*

Equations 2 to 5 were applied to the experimental data set, obtaining kinetic energy and power corresponding to distances of 3, 6, 9 and 12 m from the sprinkler. Using these data, exponential equations were built to estimate  $\delta_p$  as a function of distance from the sprinkler to a distance of 12 m. In the absence of experimental data beyond 12 m, a linear decrease in  $\delta_p$  was assumed from this point to the maximum sprinkler reach (where by definition  $\delta_p = 0 \text{ W m}^{-2}$ ).

#### *Estimated drop velocity data*

This case is based on the use of a disdrometer for drop characterization. As a consequence, only drop diameter is available for each drop in the data set. Bautista-Capetillo et al. (2009) used a disdrometer to measure 13,254 drop diameters in the same conditions used in low-

speed photography. At each pressure and distance from the sprinkler the disdrometer measured drop diameters were used, and drop velocities were derived from Eq. 1. The low-speed photography data set used in this study constituted part of the source data for the derivation of Eq. 1, although the agreement between data presented by Salvador et al. (2009) and Bautista et al. (2009) was very relevant. Kinetic energy was determined for each drop in the data set. Average values of specific power were determined for each pressure and each distance from the sprinkler. Finally, the  $\delta_p$  radial curve was obtained from a combination of exponential and linear regressions merging at a distance of 12 m.

#### *Simulated drop diameter and velocity data*

The ballistic model was used to estimate the relationship between the distance from the sprinkler and the resulting  $\delta_p$ . This process was based on the simulation of trajectory for drops of different diameters (with 0.5 mm increments) till the sprinkler reach was obtained. Simulated exponential equations were combined with a linear decrease from the peak point of specific power (12.5, 11.4 and 12.7 m for operating pressures of 200, 300 and 400 kPa, respectively) to the maximum sprinkler reach.

#### **Specific power in a sprinkler spacing: maps and uniformity**

Analysing specific power within a sprinkler spacing permits construction of power maps. Locating the areas within a sprinkler spacing having high or low specific power has relevant agronomic and irrigation management implications. In the present paper this analysis was performed for different sprinkler spacings (rectangular, R and triangular, T). Sprinkler spacings are commonly expressed by the letter R or T followed by the spacing between sprinklers within a line (m), times the spacing between the lines (m). The

sprinkler spacings considered in this work were: R15x15, R18x18, T15x15, T18x18 and T18x15. Among the considered triangular spacings, only T18x15 is an equilateral triangle, thus optimizing water application.

At a given point the overlapping of the drops supplied by all contributing sprinklers determines the received water and the resulting specific power. For the experimental conditions, in the absence of wind, these amounts depend on the operating pressure and on the sprinkler spacing. Measured, estimated and simulated specific power radial curves can be used to produce specific power maps and kinetic energy maps (if the irrigation time is known).

The sprinklers located at the vertices of Rectangular and Triangular sprinkler spacings were assigned cartesian coordinates from a datum located at the lower left corner. Each sprinkler spacing was discretized using 400 cells of equal dimensions (rectangles or triangles for rectangular or triangular spacings, respectively). The specific power applied by each sprinkler at the centre of the cell was determined using the radial curves. The total specific power at a certain point was obtained as the addition of the power applied by the four sprinklers located at the vertices of a rectangular spacing or the three sprinklers located at the vertices of a triangular spacing.

Specific power estimates were obtained at each cell for each calculation method (measured, estimated and simulated), sprinkler spacing (two rectangular spacings and three triangular spacings), and operating pressure (200, 300 and 400 kPa). Specific power maps were produced using the ordinary Kriging interpolation technique using a spherical semivariogram model. These maps permit one to characterize the spatial variability of this variable. Uniformity indexes, commonly used in irrigation analysis, were additionally

used for this purpose. Following the criteria adopted by Chistiansen (1942) to evaluate the uniformity of sprinkler irrigation systems, Merriam and Keller (1978) proposed the coefficient of uniformity (CU, %). This coefficient was applied in this work to specific power in a sprinkler spacing ( $CU_{\delta_p}$ , %). In standard irrigation evaluation procedures, a sprinkler spacing is divided into a matrix of rectangular domains with a water collector located at the centre. Collectors are used to estimate the precipitation rate at each domain. In this work, the sprinkler spacing was divided into 400 cells. As a consequence,  $CU_{\delta_p}$  can be expressed as:

$$CU_{\delta_p} = 100 \left( 1 - \frac{\sum_{i=1}^{400} |\delta_{p_i} - \bar{\delta}_p|}{400 \bar{\delta}_p} \right) \quad [7]$$

where:

$\delta_{p_i}$  is the specific power at the centre of cell  $i$  ( $W m^{-2}$ ); and

$\bar{\delta}_p$  is the average specific power on the sprinkler spacing ( $W m^{-2}$ ).

## **Results and discussion**

### **Kinetic energy and power from measured data**

Kinetic energy was determined for each of the 1,229 drops characterized during the experimental isolated irrigation sprinkler experiment. Figure 1 presents the relation between kinetic energy from measured data and drop diameter for the different operating pressures and distances to the sprinkler. Logarithmic energy axes were required, since differences in kinetic energy within the experimental range in diameters (approximately between 0.5 and 5.5 mm) approached three orders of magnitude.

The range in drop kinetic energy ( $E_{kd}$ ) was very similar for the three operating pressures at distances of 3 and 6 m from the sprinkler. Numerical values between 0.60 and 150  $10^{-7}$  J were obtained at 3 m, while at 6 m the range was 0.89 – 415  $10^{-7}$  J. On the other hand, for distances of 9 and 12 m, a clear inverse trend could be appreciated between pressure and kinetic energy. The absolute ranges for 9 and 12 m were 2.03-1,621  $10^{-7}$  J and 23.6-23,413  $10^{-7}$  J, respectively. In the experimental conditions the extreme values in drop kinetic energy increased with distance from the sprinkler and decreased with sprinkler operating pressure.

Table 1 presents the volumetric mean ( $d_V$ ) and volume median ( $d_{50}$ ) drop diameters and corresponding experimental kinetic energy ( $E_{kd}$ , J  $10^{-7}$ ). Data are presented for combinations of operating pressure and distance to the sprinkler. While  $d_V$  is the arithmetic mean diameter,  $d_{50}$  is the drop diameter corresponding to 50% cumulative drop volume. The distance-averaged differences in kinetic energy between  $d_V$  and  $d_{50}$  amounted to 1 %, 8 % and 9% of  $d_V$  for operating pressures of 200, 300 and 400 kPa, respectively. The

average drop kinetic energy clearly increased with distance from the sprinkler. Between distances of 3 m and 12 m, the respective pressure-averaged kinetic energy increased by 67 times for  $d_V$  and 88 times for  $d_{50}$ . Regarding the operating pressure, neither  $d_V$  nor  $d_{50}$  revealed a clear trend between operating pressure and  $E_{kd}$  for a distance of 3 m. An inverse relationship between operating pressure and  $E_{kd}$  became clear at distances of 6-12 m. For instance, at a distance of 12 m, increasing the operating pressure from 200 to 400 kPa resulted in a 91 % reduction of  $E_{kd}$  for  $d_V$  and a 94 % reduction of  $E_{kd}$  of  $d_{50}$ . The average kinetic energy figures confirmed the conclusions of the analysis on individual drop energy (Fig. 1).

Predictive equations are presented in Table 2 for kinetic energy estimation as a function of  $d_V$  and  $d_{50}$ . The resulting coefficients of determination ranged between 0.973 and 0.998. These equations are oriented to the estimation of kinetic energy in irrigation system design and management applications, since  $d_V$  and  $d_{50}$  are common outputs of drop characterization analyses. The equation derived using data from all three experimental pressures did not result in a decrease in the value of  $R^2$  with respect to the pressure-specific equations, in general.

Kinetic energy per unit volume ( $E_{k\Omega}$ ,  $J L^{-1}$ ) was computed from Eq. [2]. Figure 2 presents the relationship between distance from the sprinkler and sprinkler kinetic energy.  $E_{k\Omega}$  clearly increased with distance from the sprinkler, following an exponential trend. An inverse relationship could be observed between  $E_{k\Omega}$  and pressure, in general. This relationship was particularly evident for a distance of 12 m. In the rest of distances, the differences in  $E_{k\Omega}$  were much less between 200 and 300 kPa than between 300 and 400 kPa.

The decrease in drop diameter with increased pressure, particularly at 6 and 9 m (Table 1) seems to be the primary cause for this relationship.

Table 3 presents values for experimental precipitation rate, sprinkler kinetic energy per unit volume and specific power at the four measured radial locations. The values reported in this Table are comparable to the previous findings by Kincaid (1996) and DeBoer (2002) for different impact sprinklers and operating conditions, and by DeBoer and Monnens (2001) for a rotating spray plate sprinkler. The significance of these estimates was affected by the fact that only four observation points were available along the sprinkler irrigated radius. Kinetic energy per unit volume,  $E_{k\Omega}$ , increased with distance from the sprinkler and decreased with operating pressure, while  $\delta_p$  exponentially increased with distance to the sprinkler. Exponential regression equations 8, 9 and 10 were obtained for experimental specific power ( $\delta_p$ ) measured at 200, 300 and 400 kPa, respectively. In these equations, independent variable  $x$  represents the distance to the sprinkler. The coefficients of determination ( $R^2$ ) follow the equations:

$$\delta_{p\ 200kPa} = 0.000630 e^{0.262x}; \quad R^2 = 0.922 \quad [8]$$

$$\delta_{p\ 300kPa} = 0.000820 e^{0.214x}; \quad R^2 = 0.986 \quad [9]$$

$$\delta_{p\ 400kPa} = 0.00107 e^{0.179x}; \quad R^2 = 0.981 \quad [10]$$

### **Comparing specific power determined from different data sources**

Figure 3 presents radial curves of specific power derived from measured, estimated and simulated data. Notable agreement was observed between measured and estimated specific power at pressures of 200 and 300 kPa, although in specific areas of the curve and

for certain experimental pressures, errors were relevant. This is the case for the pressure of 400 kPa, in which estimated velocity resulted in severe underestimation of specific power at short distances from the sprinkler.

In contrast to measured and estimated data, simulated power data were available at distances beyond 12 m. It is interesting to note how in all three pressures simulated specific power decreased for distances exceeding approximately 12 m, and how this decrease could be assimilated to a linear trend. This observation provided validation for the hypothesis used to model specific power.

Simulated velocity resulted in a very important overestimation of specific power. While experimental data include a statistical distribution of drop diameters and velocities, simulated data are based on the drop diameter landing at each observation distance and its kinetic energy. This has a relevant effect on kinetic energy estimation, since the relationship between diameter and energy is strongly non-linear (Fig. 1). Burguete et al. (2007) described how - during the process of jet break-up and the travel of large drops - small drops are continuously formed. The formation of these drops at variable distances between the sprinkler nozzle and the sprinkler reach can not be reproduced by current ballistic sprinkler models. As a consequence, at a given distance from the sprinkler, the ballistic drop diameter at that distance represents the upper bound of drop diameter. In addition, a population of smaller drops appears at this point. This statistical distribution of drop diameters results in a specific power which is much smaller than the one corresponding to the ballistic drop diameter. Discrepancies between simulated and observed data indicate that it is important to continue experimental drop characterization and simulation model development efforts.

### **Computing and mapping specific power for different sprinkler spacings**

Figures 4 and 5 present experimentally determined contour maps of specific power under no-wind conditions for the selected rectangular and triangular sprinkler spacings. In rectangular spacings, specific power attained maximum values at the central part of the spacing, with a total range between spacings and pressures of 0.0675-0.0750 W m<sup>-2</sup> (Table 4). Areas of lower specific power appeared at the sprinkler spacing boundaries (Fig. 4). In these areas power ranged from 0.0010 to 0.0075 W m<sup>-2</sup> (Table 4). In triangular spacings, a common pattern of specific power distribution could be observed: low energy near the boundaries and often at the centre (Fig. 5). The maximum specific power did not exceed 0.0525 W m<sup>-2</sup> in triangular spacings (Table 4). Comparing the same spacings in rectangular and triangular arrangements, the highest values of specific power were obtained in rectangular arrangements.

Figure 6 reproduces some of the cases presented in Figures 4 and 5, but using estimated and simulated data. The common spacings T18x18 and R18x15 operating at 300 kPa are presented. These maps were similar to maps derived from measured variables in terms of the patterns of high and low specific power areas. However, the differences in the magnitude of specific power identified in Fig. 3 resulted in under- and overestimation of the specific power determined from experimental measurements. Despite these scale errors, estimated and simulated data succeeded in locating areas of high and low specific power.

Table 5 presents the average values of specific power in the analyzed sprinkler spacings for all three sources of data. In general, a given spacing in m x m results in the same average specific power in the R and T versions. Small numerical differences are likely due

to the non-linear nature of the first reach of the radial curve. For a given pressure, the differences in the average value of specific power are only related to the amplitude of the spacing. Data in Table 5 permits one to quantify the average errors, compared to measured powers, due to specific power estimation (underestimation by 17 %) and simulation (overestimation by 172 %).

Specific power coefficients of uniformity ( $CU_{\delta_p}$ , %) are also presented in Table 5 for the different spacings and operating pressures, using the three data sources. Theoretically adequate spacings, such as R15x15, R18x18 and T18x15 showed fair  $CU_{\delta_p}$  based on measured data at the recommended operating pressure of 300 kPa (65, 50 and 65 %, respectively). Spacing T18x18, an isosceles triangle which is favored by local farmers in Spain due to its relatively low cost and good adaptation to farm machinery, showed a reasonable  $CU_{\delta_p}$  of 47 %. Specific power uniformity (averaged across all spacings) based on measured, estimated and simulated data resulted in remarkable agreement (60 %, 53 % and 59 % on the average, respectively). Specific power uniformity nearly always increased with operating pressure. A regression analysis was performed on measured *vs.* estimated and simulated  $CU_{\delta_p}$ . The regression model could explain 90 and 99 % of the variability in estimated and simulated  $CU_{\delta_p}$ , respectively. Additionally, the regression line for simulated data could not be distinguished from a 1:1 line at a 95 % probability level (Fig. 7). An additional analysis was performed to confirm the correspondence between specific power values. Statistical correlation was assessed between paired estimates of specific power at the 400 cells, comprising measured data on one side and estimated or simulated

data on the other. Average correlation coefficients were 0.980 and 0.998 for estimated and simulated data, respectively.

## **Conclusions**

The data set containing windless experimental measurements of drop diameter and velocity has permitted us to characterize impact sprinkler kinetic energy based on measured drop diameter and velocity. Drop kinetic energy exponentially increased with drop diameter. Sprinkler kinetic energy and specific power exponentially increased with distance from the sprinkler. Empirical equations were presented to estimate drop kinetic energy from average drop diameter and to estimate specific power from distance to the sprinkler at three pressures. Measured, estimated and simulated data were used to estimate specific power. The results showed similarities between the three data sources in a number of aspects. However, simulated values largely overestimated (by 172 %) average specific power. Estimated specific power showed moderate underestimation (by 17 %) when compared with measured data.

While the ballistic simulation model produced just one drop velocity per distance to the sprinkler, the measured and estimated data sets (low-speed photography and disdrometer, respectively) contained a population of drops at each distance. Counting on just one velocity value per distance from the sprinkler is more problematic for the estimation of kinetic energy than it is for the estimation of irrigation depth, due to the strong non-linearity between drop diameter and energy. As a consequence, estimated drop data are much more valuable to reflect the adequate magnitude of drop kinetic energy and related variables than simulated drop data. The estimated data set can be considered adequate to determine kinetic energy and power variables. However, the equation used to estimate velocity from drop diameter should be further validated to assess its applicability in different conditions. Regarding low-speed photography data,

more intense (more drops) and detailed (more observation points) data sets would be required to obtain more accurate estimates.

The reported average values of measured specific power, the associated contour maps and the coefficients of uniformity can be used in combination with experimentally obtained threshold values of specific power for irrigation design and management purposes. Intense field campaigns will be required to obtain these data for a given soil-crop-irrigation combination. Our contribution to this problem is therefore more methodological than practical, since limited data sets are currently available on the impact of kinetic energy on agricultural systems. Despite the overestimation in simulated specific power, the agreement between the three  $CU_{\delta_p}$  data sets constitutes a relevant research finding.

Unfortunately, real conditions include sprinkler models and nozzle configurations different than the ones used in this research, untested values of pressure and particularly, windy conditions. In the absence of experimental values, estimated and even simulated data can be cautiously used to assess specific power distribution and uniformity under sprinkler irrigation. This will be particularly important for windy conditions, in which kinetic energy can be particularly harmful to the soil, and drop characterization efforts are still incipient. Discrepancies between simulated and observed drop data permit one to conclude that it is important to continue experimental drop characterization and simulation model development efforts. In particular, a larger experimental drop characterization data set would be required to provide firmer conclusions.

## **Acknowledgements**

This research was funded by the *Agencia Española de Cooperación Internacional para el Desarrollo* (AECID). Thanks are also due to the *Universidad Autónoma de Zacatecas*, México.

## References

- Basahi JM (1998) A piezoelectric film sensor improvement and evaluation for measuring water droplet impact energy and determining droplet impact effects on soil surfaces. Doctoral Dissertation, Texas A&M University
- Bautista-Capetillo CF, Salvador R, Burguete J, Montero J, Tarjuelo JM, Zapata N, Gonzalez J, Playan E (2009) Comparing methodologies for the characterization of water drops emitted by an irrigation sprinkler. *Transactions of the ASABE* 52(5): 1493-1504.
- Burguete J, Playán E, Montero J, Zapata N (2007) Improving drop size and velocity estimates of an optical disdrometer: implications for sprinkler irrigation simulation. *Transactions of the ASABE*, 50(6): 2103-2116.
- Carrión P, Tarjuelo JM, Montero J (2001) SIRIAS: a simulation model for sprinkler irrigation. I Description of model. *Irrigation Science* 20: 73-84.
- Christiansen JE (1942) *Irrigation by Sprinkling*. University of California. Agricultural Experimental Station, Bulletin 670, 124 pp.
- Cruvinel PE, Minatel ER, Mucheroni ML, Vieira SR, Crestana S (1996) An automatic method based on image processing for measurements of drop size distribution from agricultural sprinklers. *Anais do IX SIBIGRAPI*, 39-46.
- Cruvinel PE, Vieira SR, Crestana S, Minatel ER, Mucheroni ML, Neto AT (1999) Image processing in automated measurements of raindrop size and distribution. *Computers and Electronics in Agriculture* 23: 205-217.
- De Wrachien D, Lorenzini G (2006) Modelling jet flow and losses in sprinkler irrigation: Overview and perspective of a new approach. *Biosystems Eng.* 94(2): 297-309.

- DeBoer DW 2002 Drop and energy characteristics of a rotating spray-plate sprinkler. *Journal of Irrigation and Drainage Engineering*, ASCE 128(3): 137-146.
- DeBoer DW, Monnens MJ (2001) Estimation of drop size and kinetic energy from a rotating spray-plate sprinkler. *Transactions of the ASAE* 44(6): 1571-1580.
- Dechmi F, Playán E, Cavero J, Martínez-Cob A, Faci JM (2004a) A coupled crop and solid set sprinkler simulation model: I. Model development. *Journal of Irrigation and Drainage Engineering*, ASCE 130(6): 499-510.
- Dechmi F, Playán E, Cavero J, Martínez-Cob A, Faci JM (2004b) A coupled crop and solid set sprinkler simulation model: II. Model application. *Journal of Irrigation and Drainage Engineering*, ASCE 130(6): 511-519.
- Duley FL (1939) Surface factors affecting the rate of intake of water by soil. *Soil Science Society American Proceedings* 4:60-64.
- Eigel JD, Moore ID (1983) A simplified technique for measuring raindrop size and distribution. *Trans Am Soc Agric Eng* 26(4): 1079-1084.
- Ellison WD (1947) Some effects of erosion on infiltration and surface runoff. *Agricultural Engineering* 28(6): 245-249
- Fukui Y, Nakanishi K, Okamura S (1980) Computer evaluation of sprinkler irrigation uniformity. *Irrigation Science* 2: 23-32.
- Hauser D, Amayenc P, Nutten B, Waldteufel P (1984) A new optical instrument for simultaneous measurement of raindrop diameter and fall speed distributions. *J At Ocean Technol* 1(3): 256-269.

- Jones DMA (1956) Rainfall drop-size distribution and radar reflectivity. Illinois state water survey, Meteorology Laboratory, research report no. 6, 20 pp.
- Joss J, Waldvogel (1967) Ein Spectrograph für Niederschlagstropfen mit automatischer Auswertung (A spectrograph for the automatic analysis of raindrops). Pure Appl Geophys 68: 240-246.
- Kincaid DC (1996) Spraydrop kinetic energy from irrigation sprinklers. Transactions of the ASAE 39(3): 847-853.
- Kincaid DC, Solomon KH, Oliphant JC (1996) Drop size distributions for irrigation sprinklers. Transactions of the ASAE 39(3): 839-845.
- King BA, Bjorneberg DL (2010) Characterizing droplet kinetic energy applied by moving spray-plate center-pivot irrigation sprinklers. Transactions of the ASABE 53(1): 137-145
- King BA, Winward TW, Bjorneberg DL (2010) Laser precipitation monitor for measurement of drop size and velocity of moving spray-plate sprinklers. Applied Engineering in Agriculture. 26(2): 263-271.
- Kohl RA, DeBoer DW, (1984) Drop size distributions for a low pressure spray type agricultural sprinkler. Trans Am Assoc Agric Eng 27(6): 1836-1840.
- Kohl RA, DeBoer DW, Evenson PD (1985) Kinetic energy of low pressure spray sprinklers. Transactions of the ASAE 28(5):1526-1529.
- Lehrsch GA, Kincaid DC (2010) Sprinkler irrigation effects on infiltration and near-surface unsaturated hydraulic conductivity. Transactions of ASABE 53(2): 397-404.
- Li J, Kawano H (1995) Simulating water-drop movement from noncircular sprinkler nozzles. J. Irrigation and Drainage Division, ASCE 121: 152-158.

- Magarvey RH (1956) Stain method of drop size determination. *J Meteorol* 14: 182-184
- Merriam JL, Keller J (1978) *Farm irrigation system evaluation: A guide for management*. Utah State University, Logan, Utah, USA. 271 pp.
- Mohammed D, Kohl RA (1987) Infiltration response to kinetic energy. *Transactions of ASAE* 30(1): 108-111.
- Montero J, Tarjuelo JM, Carrión P (2003) Sprinkler droplet size distribution measured with an optical spectropuviometer. *Irrigation Science* 22: 47-56.
- Okamura S (1968) Theoretical study on sprinkler sprays. *Transactions JSIDRE* 26: 49-55.
- Park, SW, Mitchell, JK, Budenzer, GD (1982). Splash erosion modeling: physical analysis. *Transactions of the ASAE* 25(2): 357-361.
- Playán E, Zapata N, Faci JM, Tolosa D, Lacueva JL, Pelegrín J, Salvador R, Sánchez I, Lafita A (2006) Assessing sprinkler irrigation uniformity using a ballistic simulation model. *Agricultural Water Management* 84: 86-100.
- Press WH, Flannery BP, Teukolsky SA, Vetterling WT (1988) *Numerical recipes in C*. Cambridge University Press, 735 pp.
- Salles C, Poesen J, Borselli L (1999) Measurement of simulated drop size distribution with an optical spectro-pluviometer: sample size considerations. *Earth Surface Processes Landforms* 24(6): 545-556.
- Salvador R, Bautista-Capetillo C, Burguete J, Zapata N, Playán E (2009). A photographic methodology for drop characterization in agricultural sprinklers. *Irrigation Science* 27(4): 307-317.

Seginer I (1965) Tangential velocity of sprinkler drops. Transactions of the ASAE 90-93.

Sudheer KP, Panda RK (2000) Digital image processing for determining drop sizes from irrigation spray nozzles. Agricultural Water Management, 45 159-167.

Thompson AL, James LG (1985) Water droplet impact and its effect on infiltration. Transactions of the ASAE 28(5): 1506-1510.

Vories ED, von Bernuth RD, Mickelson RH (1987) Simulating sprinkler performance in wind. J. Irrigation and Drainage Division, ASCE 113(1): 119-130.

Wiesner J (1895) Beiträge zur Kenntniss der Größe des tropischen Regens. Akademie der Wissenschaften, Mathematika-Naturwissenschaften Klasse, vol. 104: 1397-1434. Berlin, Germany. Sitz Berlin Verlag.

## **List of Tables**

**Table 1.** *Drop kinetic energy ( $E_{kd}$ , J  $10^{-7}$ ) from measured drop data. Results correspond to different values of average drop diameter ( $d_V$  and  $d_{50}$ ) and to combinations of operating pressure and distance to the sprinkler in the experimental data set.*

**Table 2.** *Predictive equations for measured drop kinetic energy ( $E_{kd}$ , J  $10^{-7}$ ) using the volumetric mean diameter ( $d_V$ , mm) and the volume median diameter ( $d_{50}$ , mm) as independent variables.*

**Table 3.** *Precipitation rate ( $R$ ), sprinkler kinetic energy ( $E_{k\Omega}$ ) and specific power ( $\delta_p$ ) obtained from measured data for combinations of operating pressure and distance to the sprinkler.*

**Table 4.** *Area (both in  $m^2$  and in % of the sprinkler spacing area) within specified intervals of measured specific power for different sprinkler spacings and operating pressures.*

**Table 5.** *Average specific power ( $\delta_p$ ) and coefficient of uniformity of specific power for combinations of sprinkler spacing and operating pressure. Results are presented for measured, estimated and simulated drop data.*

## **List of Figures**

**Figure 1.** Scatter plots of drop diameter (mm) vs. drop kinetic energy ( $E_{kd}$ , J  $10^{-7}$ ) for the combinations of operating pressure and distance to the sprinkler in the experimental data set.

**Figure 2.** Sprinkler kinetic energy ( $E_{k\Omega}$ ) from measured data. Results are presented as a function of distance to the sprinkler for the three considered operating pressures.

**Figure 3.** Specific power ( $\delta_p$ ) as a function of distance to the sprinkler for the three considered operating pressures. Results are presented from measured, estimated and simulated data.

**Figure 4.** Contour maps of specific power ( $\delta_p$ ) from measured data. Results are presented for combinations of rectangular sprinkler spacings and operating pressures.

**Figure 5.** Contour maps of specific power ( $\delta_p$ ) from measured data. Results are presented for combinations of triangular sprinkler spacings and operating pressure.

**Figure 6.** Contour map of estimated and simulated kinetic power ( $\delta_p$ ) for spacings R18x18 and T18x15 operating at 300 kPa.

**Figure 7.** Scatter plot of measured  $CU_{\delta_p}$  vs. simulated and estimated  $CU_{\delta_p}$ . Regression lines, equations and coefficients of determination ( $R^2$ ) are presented for both dependent variables.

**Table 1.** Drop kinetic energy ( $E_{kd}$ , J  $10^{-7}$ ) from measured drop data. Results correspond to different values of average drop diameter ( $d_V$  and  $d_{50}$ ) and to combinations of operating pressure and distance from the sprinkler in the experimental data set.

Pressure (kPa)		Distance from the sprinkler			
		3 m	6 m	9 m	12 m
200	$d_V$ (mm)	1.12	1.48	1.93	3.28
	$E_{kd}$ (J $10^{-7}$ )	27.2	79.5	330	3337
	$d_{50}$ (mm)	1.05	1.40	1.92	3.59
	$E_{kd}$ (J $10^{-7}$ )	22.4	67.3	325	4375
300	$d_V$ (mm)	1.08	1.43	1.44	2.65
	$E_{kd}$ (J $10^{-7}$ )	19.8	65.3	114	1282
	$d_{50}$ (mm)	1.06	1.40	1.39	2.55
	$E_{kd}$ (J $10^{-7}$ )	18.7	61.3	103	1142
400	$d_V$ (mm)	1.19	1.25	1.46	1.78
	$E_{kd}$ (J $10^{-7}$ )	26.1	44.8	113	288
	$d_{50}$ (mm)	1.17	1.18	1.42	1.73
	$E_{kd}$ (J $10^{-7}$ )	24.8	37.7	104	265

**Table 2.** Predictive equations for measured drop kinetic energy ( $E_{kd}$ , J  $10^{-7}$ ) using the volumetric mean diameter ( $d_v$ , mm) and the volume median diameter ( $d_{50}$ , mm) as independent variables.

Operating pressure (kPa)	Kinetic energy (J)	R <sup>2</sup>
200	$E_k = \frac{d_v^{4.553}}{500000}$	0.997
	$E_k = \frac{d_{50}^{4.350}}{500000}$	0.998
300	$E_k = \frac{d_v^{4.592}}{500000}$	0.982
	$E_k = \frac{d_{50}^{4.616}}{500000}$	0.980
400	$E_k = \frac{d_v^{5.578}}{1000000}$	0.983
	$E_k = \frac{d_{50}^{5.671}}{1000000}$	0.973
All	$E_k = \frac{d_v^{4.624}}{500000}$	0.985
	$E_k = \frac{d_{50}^{4.486}}{500000}$	0.984

**Table 3.** Precipitation rate ( $R$ ), sprinkler kinetic energy ( $E_{k\Omega}$ ) and specific power ( $\delta_p$ ) obtained from measured data for combinations of operating pressure and distance to the sprinkler.

Operating pressure (kPa)	Distance from sprinkler (m)	Precipitation rate (mm h <sup>-1</sup> )	Sprinkler kinetic energy (J L <sup>-1</sup> )	Specific power (W m <sup>-2</sup> )
200	3	1.46	4.45	0.0018
	6	1.21	6.89	0.0023
	9	1.66	11.49	0.0053
	12	3.17	21.36	0.0188
300	3	1.66	3.69	0.0017
	6	1.66	5.96	0.0027
	9	2.13	8.85	0.0052
	12	2.60	16.07	0.0116
400	3	1.88	3.65	0.0019
	6	1.83	5.53	0.0028
	9	2.42	8.88	0.0060
	12	2.62	12.15	0.0088

**Table 4.** Area (both in m<sup>2</sup> and in % of the sprinkler spacing area) within specified intervals of measured specific power for different sprinkler spacings and operating pressures.

Operating Pressure (kPa)	Range of specific power (W m <sup>-2</sup> )		Sprinkler spacing (Rectangular/Triangular, mxm)									
			R 15x15		R 18x18		T 15x15		T 18x18		T 18x15	
			Area (m <sup>2</sup> )	Area (%)	Area (m <sup>2</sup> )	Area (%)	Area (m <sup>2</sup> )	Area (%)	Area (m <sup>2</sup> )	Area (%)	Area (m <sup>2</sup> )	Area (%)
200	0.0010	0.0075	6.00	2.67	62.00	19.14	7.50	6.67	43.00	26.54	25.00	18.52
	0.0075	0.0150	61.00	27.11	36.00	11.11	10.50	9.33	19.00	11.73	13.00	9.63
	0.0150	0.0225	36.00	16.00	112.00	34.57	17.00	15.11	35.00	21.60	27.00	20.00
	0.0225	0.0300	28.00	12.44	59.00	18.21	43.00	38.22	27.00	16.67	23.00	17.04
	0.0300	0.0375	44.00	19.56	19.00	5.86	34.50	30.67	16.00	9.88	31.00	22.96
	0.0375	0.0450	27.00	12.00	8.00	2.47	--	--	10.00	6.17	16.00	11.85
	0.0450	0.0525	19.00	8.44	9.00	2.78	--	--	12.00	7.41	--	--
	0.0525	0.0600	4.00	1.78	7.00	2.16	--	--	--	--	--	--
	0.0600	0.0675	--	--	5.00	1.54	--	--	--	--	--	--
0.0675	0.0750	--	--	7.00	2.16	--	--	--	--	--	--	
300	0.0010	0.0075	--	--	37.00	11.42	5.00	4.44	30.00	18.52	12.00	8.89
	0.0075	0.0150	37.00	16.44	98.00	30.25	9.00	8.00	26.00	16.05	9.00	6.67
	0.0150	0.0225	40.00	17.78	86.00	26.54	41.50	36.89	43.00	26.54	28.00	20.74
	0.0225	0.0300	46.00	20.44	38.00	11.73	38.00	33.78	28.00	17.28	49.00	36.30
	0.0300	0.0375	62.00	27.56	23.00	7.10	15.00	13.33	26.00	16.05	30.00	22.22
	0.0375	0.0450	33.00	14.67	16.00	4.94	4.00	3.56	9.00	5.56	7.00	5.19
	0.0450	0.0525	7.00	3.11	9.00	2.78	--	--	--	--	--	--
	0.0525	0.0600	--	--	6.00	1.85	--	--	--	--	--	--
	0.0600	0.0675	--	--	6.00	1.85	--	--	--	--	--	--
0.0675	0.0750	--	--	5.00	1.54	--	--	--	--	--	--	
400	0.0010	0.0075	--	--	21.00	6.48	--	--	18.00	11.11	5.00	3.70
	0.0075	0.0150	10.00	4.44	85.00	26.23	5.00	4.44	23.00	14.20	8.00	5.93
	0.0150	0.0225	38.00	16.89	92.00	28.40	43.00	38.22	38.00	23.46	32.00	23.70
	0.0225	0.0300	52.00	23.11	49.00	15.12	45.00	40.00	38.00	23.46	61.00	45.19
	0.0300	0.0375	88.00	39.11	31.00	9.57	17.50	15.56	40.00	24.69	23.00	17.04
	0.0375	0.0450	37.00	16.44	17.00	5.25	2.00	1.78	5.00	3.09	6.00	4.44
	0.0450	0.0525	--	--	13.00	4.01	--	--	--	--	--	--
	0.0525	0.0600	--	--	9.00	2.78	--	--	--	--	--	--
	0.0600	0.0675	--	--	4.00	1.23	--	--	--	--	--	--
0.0675	0.0750	--	--	3.00	0.93	--	--	--	--	--	--	

**Table 5.** Average specific power ( $\delta_p$ ) and coefficient of uniformity of specific power for combinations of sprinkler spacing and operating pressure.

Results are presented for measured, estimated and simulated drop data.

	Operating Pressure (kPa)	Average specific power (W m <sup>-2</sup> )					Coefficient of uniformity of specific power (%)				
		Sprinkler spacing (Rectangular / Triangular, mxm)					Sprinkler spacing (Rectangular / Triangular, mxm)				
		R 15x15	R 18x18	T 15x15	T 18x18	T 18x15	R 15x15	R 18x18	T 15x15	T 18x18	T 18x15
Measured	200	0.025	0.017	0.024	0.017	0.021	53.20	49.40	69.40	38.00	49.30
	300	0.026	0.018	0.024	0.018	0.022	65.10	50.10	75.00	47.00	65.00
	400	0.029	0.021	0.025	0.021	0.024	74.80	53.70	77.20	57.90	74.30
Estimated	200	0.024	0.017	0.024	0.017	0.020	48.30	41.60	63.70	32.10	45.50
	300	0.026	0.019	0.024	0.018	0.022	62.50	43.50	69.60	42.90	62.10
	400	0.015	0.011	0.013	0.011	0.013	67.30	39.70	61.00	49.70	64.20
Simulated	200	0.040	0.028	0.040	0.028	0.034	53.20	49.30	69.40	38.00	49.30
	300	0.082	0.058	0.076	0.058	0.069	63.90	46.90	72.40	45.00	64.00
	400	0.092	0.067	0.078	0.067	0.077	73.20	50.60	73.80	56.10	72.00

**Figure 1.** Scatter plots of drop diameter,  $d$  (mm) vs. drop kinetic energy,  $E_{kd}$  ( $J 10^{-7}$ ) for the combinations of operating pressure and distance from the sprinkler in the experimental data set.

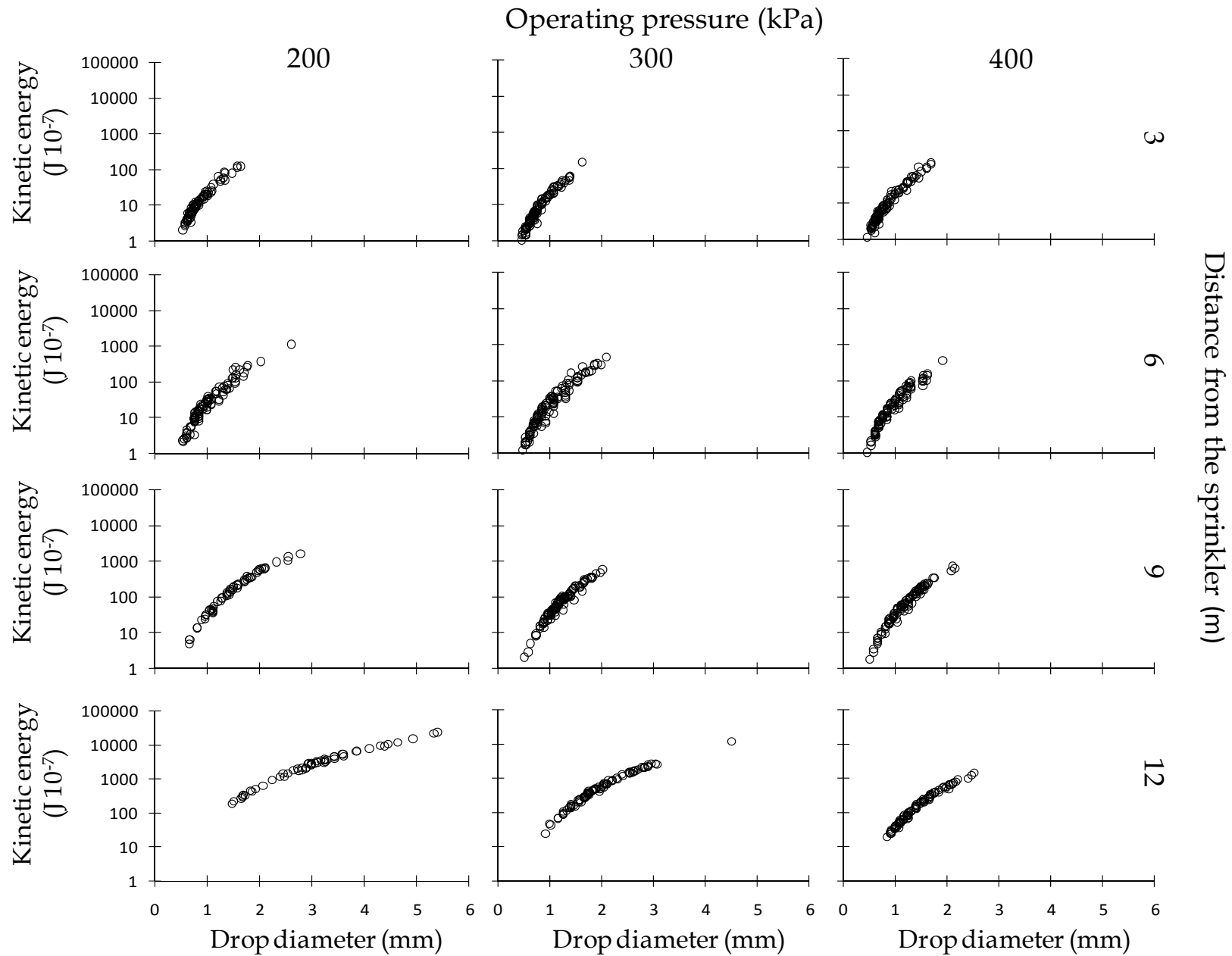


**Figure 2.** Sprinkler kinetic energy ( $E_{k\Omega}$ ) from measured data. Results are presented as a function of distance from the sprinkler for the three considered operating pressures.

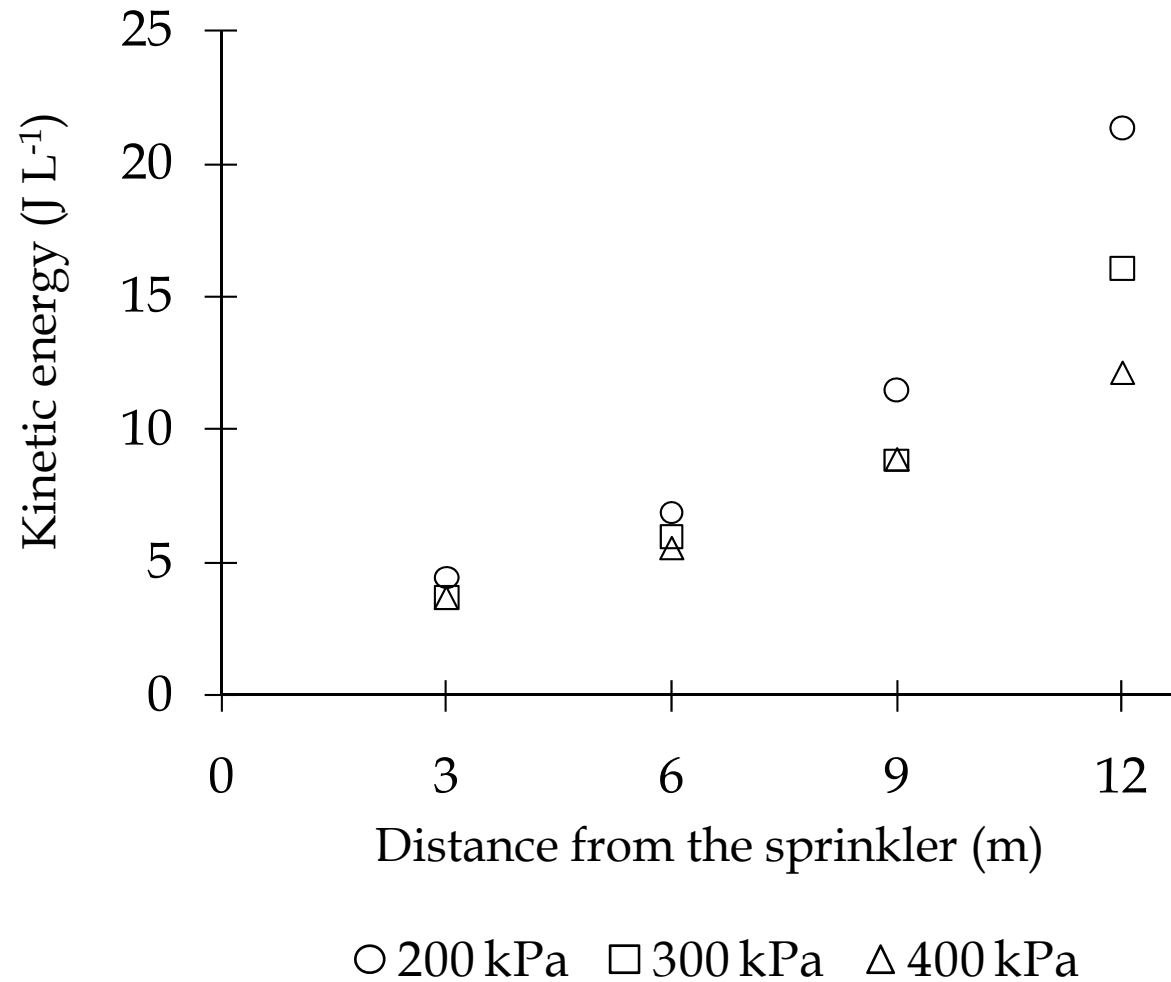


**Figure 3.** Specific power ( $\delta_p$ ) as a function of distance from the sprinkler for the three considered operating pressures. Results are presented from measured, estimated and simulated data.

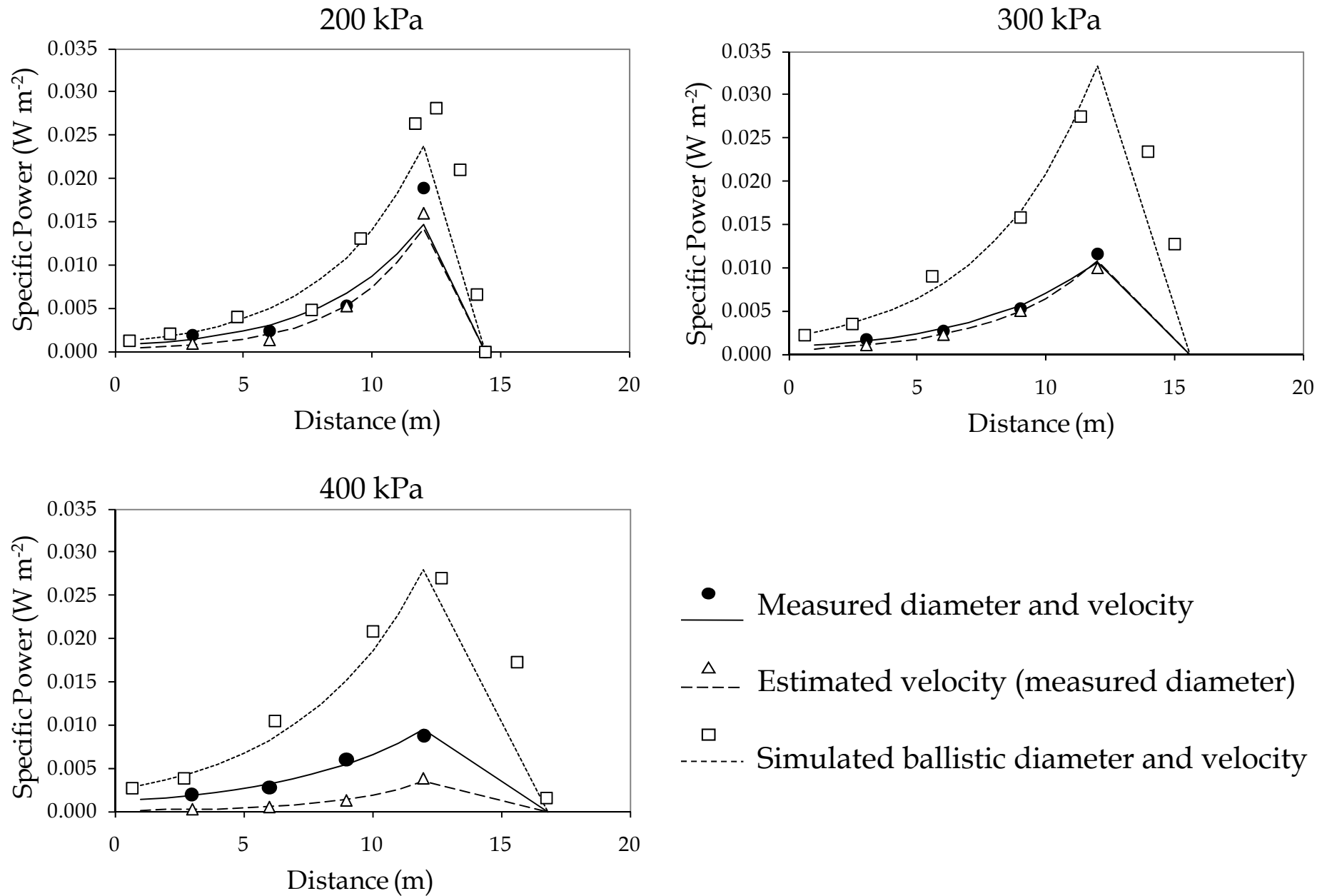


**Figure 4.** Contour maps of specific power ( $\delta_p$ ) from measured data. Results are presented for combinations of rectangular sprinkler spacings and operating pressures.

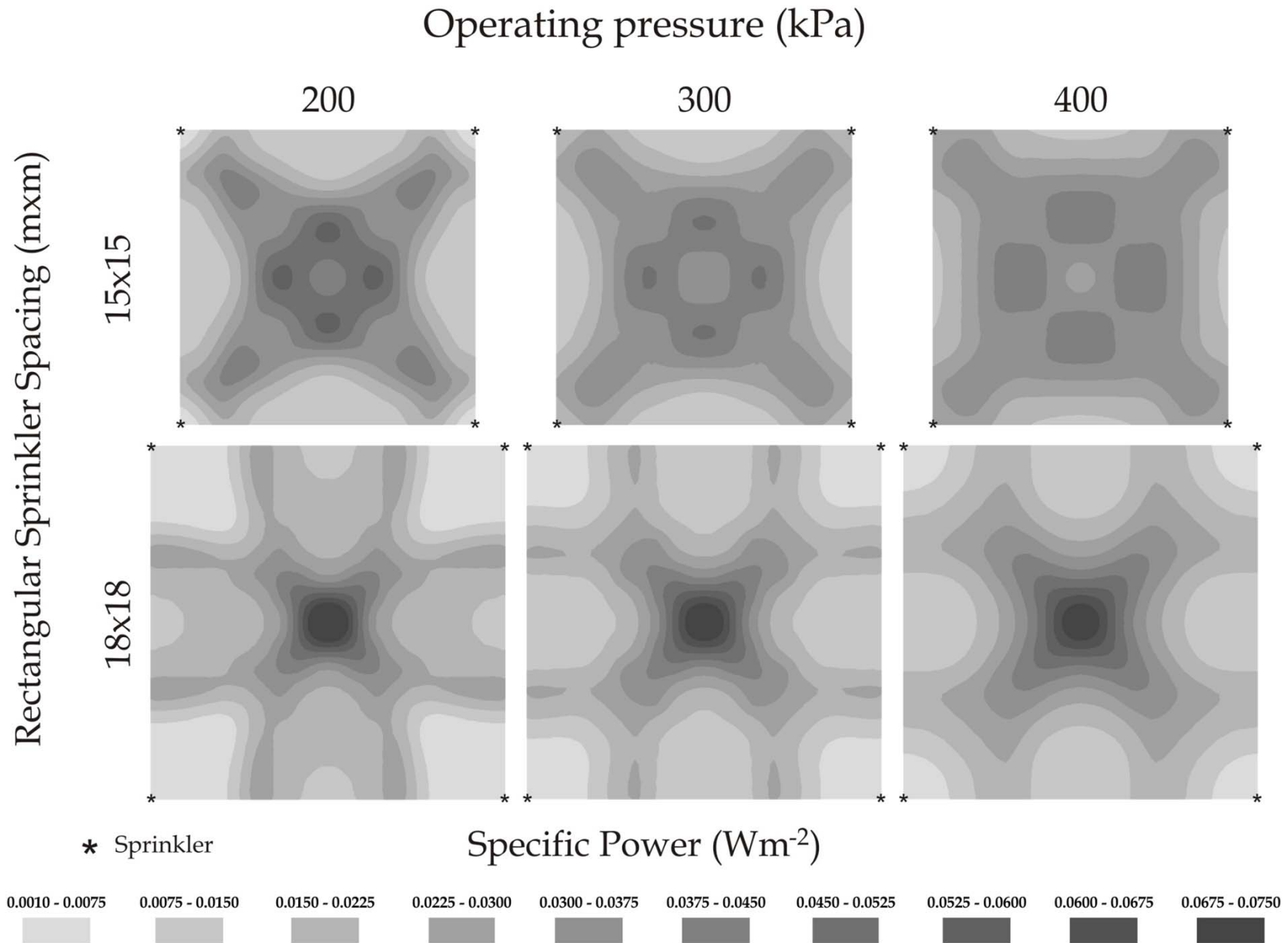


**Figure 5.** Contour maps of specific power ( $\delta_p$ ) from measured data. Results are presented for combinations of triangular sprinkler spacings and operating pressure.

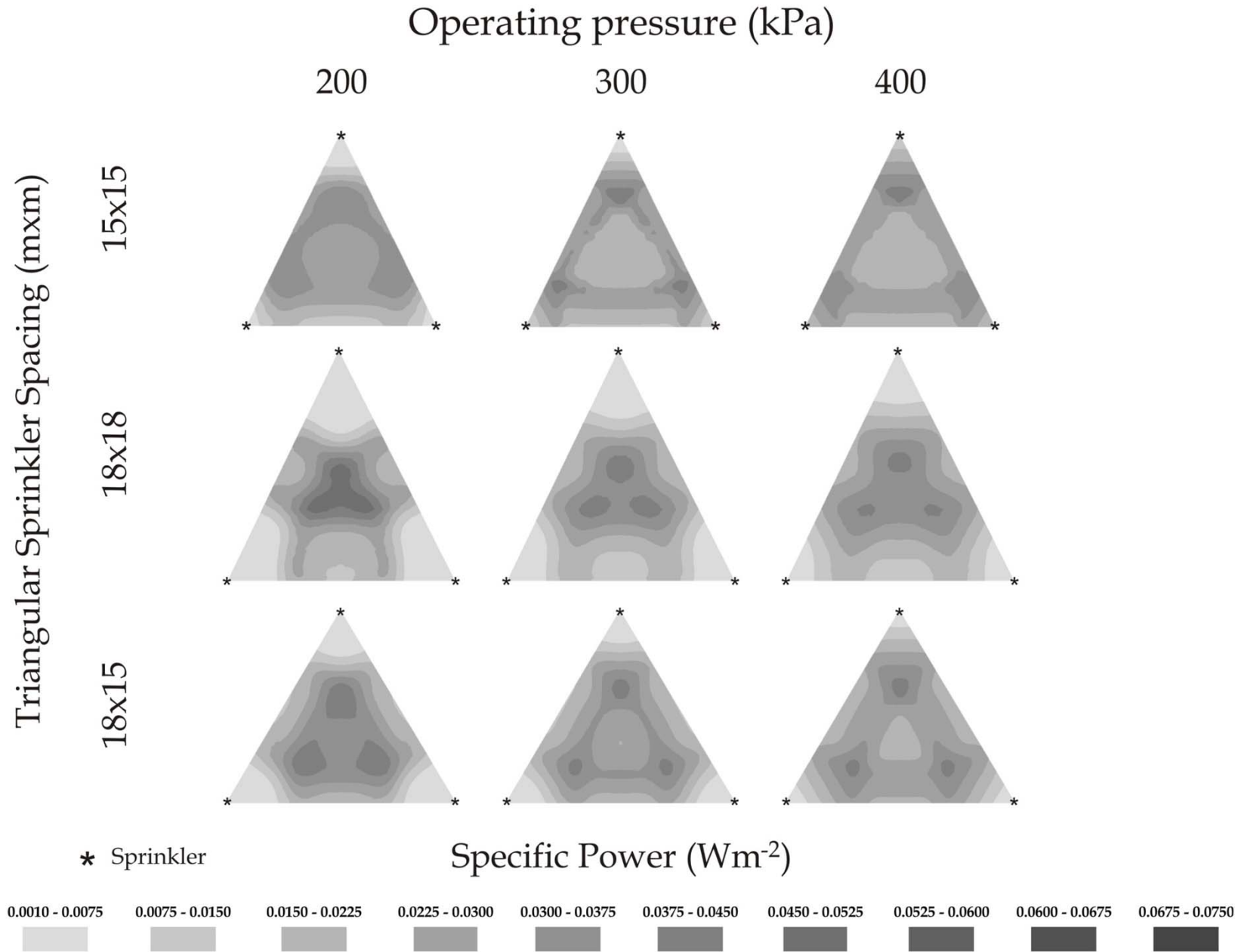




**Figure 7.** Scatter plot of measured  $CU_{\delta_p}$  vs. simulated and estimated  $CU_{\delta_p}$ . Regression lines, equations and coefficients of determination ( $R^2$ ) are presented for both dependent variables.

